

UC Berkeley

UC Berkeley Previously Published Works

Title

Long-Term Live-Cell STED Nanoscopy of Primary and Cultured Cells with the Plasma Membrane HIDE Probe Dil-SiR

Permalink

<https://escholarship.org/uc/item/1hq332ms>

Journal

Angewandte Chemie International Edition, 56(35)

ISSN

1433-7851

Authors

Thompson, Alexander D
Omar, Mitchell H
Rivera-Molina, Felix
[et al.](#)

Publication Date

2017-08-21

DOI

10.1002/anie.201704783

Peer reviewed



Published in final edited form as:

Angew Chem Int Ed Engl. 2017 August 21; 56(35): 10408–10412. doi:10.1002/anie.201704783.

Long-Term Live-Cell STED Nanoscopy of Primary and Cultured Cells with the Plasma Membrane HIDE Probe DiI-SiR

Alexander D. Thompson^[a], Mitchell H. Omar^[b], Dr. Felix Rivera-Molina^[c], Zhiqun Xi^[c], Prof. Dr. Anthony J. Koleske^[b], Prof. Dr. Derek K. Toomre^[c], and Prof. Dr. Alanna Schepartz^[a]

^[a]Department of Chemistry, Yale University 225 Prospect Street, New Haven CT 06511 (USA)

^[b]Department of Molecular Biophysics and Biochemistry and Interdepartmental Neuroscience Program, Yale University 333 Cedar Street, New Haven CT 06511 (USA)

^[c]Department of Cell Biology, Yale University 333 Cedar Street, New Haven CT 06511 (USA)

Abstract

Super-resolution imaging of live cells over extended time periods with high temporal resolution requires high-density labeling and extraordinary fluorophore photostability. Here we achieve this goal by combining the attributes of the high-density plasma membrane probe DiI-TCO and the photostable STED dye SiR-Tz. These components undergo rapid tetrazine ligation within the plasma membrane to generate the HIDE probe DiI-SiR. Using DiI-SiR, we visualized filopodia dynamics in HeLa cells over 25 min at 0.5 sec temporal resolution, and visualized dynamic contact-mediated repulsion events in primary mouse hippocampal neurons over 9 min at 2 sec temporal resolution. HIDE probes such as DiI-SiR are non-toxic and do not require transfection, and their apparent photostability significantly improves the ability to monitor dynamic processes in live cells at super-resolution over biologically relevant timescales.

Keywords

super-resolution microscopy; fluorophores; bioorthogonal chemistry; membranes; neurons

Super-resolution microscopy (nanoscopy) techniques allow fluorescence microscopes to surpass the Abbe diffraction limit[1] and visualize structural features within cells with dimensions in the tens of nanometers.[2] But obtaining super-resolution images of live cells over long time periods (tens of minutes) remains a challenge[3] because: (1) the fluorophores in most samples are fused to proteins that are present at low density[4]; and (2) most fluorophores possess limited photostability and are inactivated within seconds. Fluorophore stability is a special concern for Stimulated Emission Depletion (STED) nanoscopy[5] because the sample is co-irradiated with an exceptionally powerful depletion laser.[2] We recently described a lipid-based strategy to visualize organelle structure and dynamics within live cells at super-resolution that is compatible with both STED[6] and Single Molecule Switching (SMS)[7] nanoscopy methods and overcomes both limitations. Prolonged, live-cell confocal and STED imaging of Golgi[6] structure and dynamics was

achieved previously by combining the trans-cyclooctene (TCO)-containing high-density ceramide lipid probe Cer-TCO with the tetrazine-tagged near-IR dye SiR-Tz;[8] prolonged SMS nanoscopy[9] of multiple organelles was achieved by combining an organelle-specific, high-density lipid-TCO probe with the spontaneously blinking silicon-rhodamine dye HMSiR-Tz.[10] In the latter case, images of live cells could be acquired for tens of minutes using SMS nanoscopy because the lipid environment effectively hides most chromophores in a dark state equilibrium reservoir and protects them from photobleaching; we refer to these reagents as High-Density Environment-Sensitive (HIDE) probes.

Here we extend the utility of this lipid-based strategy to achieve long time-lapse 2D imaging of the plasma membrane of cultured cells and primary neurons using STED nanoscopy. We find that the previously reported high-density lipid probe DiI-TCO, which localizes to the plasma membrane,[9] reacts readily with SiR-Tz[6] to form the HIDE probe DiI-SiR and enables live-cell STED imaging of HeLa cells (Figure 1) for up to 25 min with 0.5 sec temporal resolution, corresponding to ~3000 time points, more than 70-fold longer than possible with Cer-SiR.[6] We highlight the simplicity and versatility of imaging with DiI-SiR by observing the dynamics of day in vitro (DIV) 4 mouse hippocampal neurons for more than 9 min. To the best of our knowledge, these two movies represent the longest live-cell STED movies of the plasma membrane in HeLa and primary neuronal cells with 2 sec temporal resolution. We anticipate that HIDE probes such as DiI-SiR will facilitate increasingly detailed, long-term studies of the biogenesis, maintenance, and function of the plasma membrane.

The membrane probe DiI-TCO was synthesized as described previously,[9] its fluorescence spectra characterized, and its reaction with SiR-Tz within the plasma membrane to generate DiI-SiR was verified using confocal microscopy (Figure 2, Supplementary Figure 1). HeLa cells transiently expressing the fluorescent plasma membrane marker VAMP2-pH[11] were treated at 37 °C with DiI-TCO (10 μ M) for 3 min followed by SiR-Tz (2 μ M) for 30 min (Figure 2a) and imaged using a confocal microscope. As expected, cells treated with 2 μ M SiR-Tz alone only show plasma membrane fluorescence due to VAMP2-pH (Figure 2b) with no significant signal in the SiR channel (Figure 2c). When cells are treated with both DiI-TCO and SiR-Tz, however, significant plasma membrane fluorescence that colocalizes with VAMP2-pH is observed in the SiR channel (Figure 2c, d). VAMP2-pH-associated fluorescence was unaffected by the presence of 10 μ M DiI-TCO (Supplementary Figure 2). Additionally, DiI-SiR did not significantly affect plasma membrane fluidity, and HeLa cells labeled with DiI-SiR continued to divide for more than 12 h (Supplementary Figure 3, 4, Supplementary Movie 1), highlighting the lack of toxicity of this lipid-based labeling method.

To evaluate the performance of DiI-SiR in live-cell STED nanoscopy, we imaged HeLa cells using a commercial Leica SP8 STED microscope equipped with a live-cell chamber that maintained the sample in an atmosphere of 5% CO₂ at 37 °C. Cells were treated with 10 μ M DiI-TCO followed by 2 μ M SiR-Tz as described above and imaged (Figure 3). Under these conditions, we observed robust plasma membrane labeling and could resolve individual filopodia with a full width at half maximum (FWHM) of 188 ± 22 nm, roughly half the value measured by confocal (366 ± 38 nm) (Figure 3a, b). Moreover, with DiI-SiR, plasma

membrane dynamics could be visualized over an extended time period—20 min—with a 2 s temporal resolution. During this time, filopodia could be seen extending, retracting, and moving laterally (Figure 3c, Supplementary Movie 2). Additionally, by decreasing the field of view to $10.57 \mu\text{m}^2$ from $19.38 \mu\text{m}^2$, we could increase our acquisition rate to 2 frames/sec (0.5 sec temporal resolution) while observing plasma membrane dynamics for 25 min—3000 frames in total (Supplementary Figure 5, Supplementary Movie 3).

To highlight the advantages of the HIDE probe DiI-SiR for STED nanoscopy of the plasma membrane, we compared the images obtained by visualizing DiI-SiR to those obtained by visualizing SiR-labeled Smo-Halo[12], a widely used plasma membrane protein marker.[13] HeLa cells expressing Smo-Halo[12] were treated with $2 \mu\text{M}$ SiR-CA[8] for 30 min at 37°C to form Smo-SiR and visualized on the Leica SP8 STED microscope (Figure 4a, Supplementary Figure 6). Under STED conditions, the Smo-SiR signal could be visualized for <1 min before significant bleaching occurred (Figure 4b, Supplementary Movie 4). Notably, cells labeled with DiI-TCO followed by SiR-Tz (Figure 4a) and imaged under the same STED conditions exhibited strong fluorescence for more than 25 min (Figure 4c, Supplementary Movie 5). Plots of the normalized fluorescence intensity over time of cells labeled with Smo-SiR revealed a half-life of 0.44 ± 0.03 min and no image could be observed after 1.5 min. Cells labelled with DiI-SiR exhibited only a $33 \pm 3\%$ decrease in fluorescence over the course of the 25 min image acquisition (Figure 4d). Taken together, these data highlight the advantages of DiI-SiR over conventional protein labeling for live-cell STED microscopy of the plasma membrane. The combination of a high labeling density with a dark state reservoir enable exceptionally long time-lapse analysis of plasma membrane dynamics with high temporal resolution.

In addition to an increase in apparent photostability, a second novel advantage of the HIDE approach is that it obviates transfection, as the reagents are simply added to live cells. To highlight this advantage, we asked whether DiI-SiR would facilitate STED nanoscopy of primary neurons of the central nervous system (CNS). Primary CNS neurons contain fine structures, such as dendritic spines and axons, and during developmental circuit formation, they also contain transient and dynamic filopodia that survey the environment and initiate synaptogenesis.[14] Because of the functional importance of these dynamic events, CNS neurons are a popular target for both live-cell STED[15] and SMS[16] nanoscopy. However, capturing transient or dynamic structures and phenomena at high spatial and temporal resolution on the time scale of minutes can be difficult with existing nanoscopy strategies. [17]

We isolated and plated mouse hippocampal neurons from <1 day-old pups under standard conditions. After 4 days, neurons were incubated at 37°C with $10 \mu\text{M}$ DiI-TCO (3 min) followed by $2 \mu\text{M}$ SiR-Tz (30 min) (Figure 5a) and subsequently imaged on a Leica SP8 STED microscope equipped with a live-cell chamber. The images revealed strong membrane fluorescence that could resolve individual filopodia on neurites with a FWHM as low as 90 nm, a greater than 4-fold improvement over confocal alone (390 nm) (Figure 5b). DiI-SiR allowed filopodia dynamics to be visualized for over 9 min at 2 sec temporal resolution (Supplementary Movie 6). Although longer movies (10–60 min) have been recorded using STED or SMS nanoscopy, their temporal resolution is poorer (11–900 sec);[15c–j, 16c, 16d]

movies with comparable or lower temporal resolution are significantly shorter (10–44 sec). [15a, 15b, 16a, 16b]

The ability to follow neuronal dynamics over long times at high temporal resolution revealed interesting behavior. In one example, we observed a pair of filopodia contacting each other at 20 sec then retracting at 60 sec (Figure 5c) followed by extension of an adjacent filopodia and another contact event at 90–132 sec (Supplementary Movie 7). We also observed filopodia undergoing likely contact-mediated repulsion[18] over the course of 158–186 sec with extension, brief contact, and rapid retraction (Figure 5d and Supplementary Movie 8). Interestingly, these events do not lead to lasting fusion, suggesting unfavorable partnering. These filopodia originate from the same cell (Supplementary Figure 7) and thus this behavior could represent a self-avoidance event that ensures the dendrites do not cross, or a self/nonself discrimination event controlling synaptic partner selection.[19] DiI-SiR enabled us to capture several additional types of dynamic neurites during the dendritic outgrowth stage of hippocampal neuron development, including dynamic dendritic branches proximal to the cell body (Supplementary Movie 9), putative spine precursor along a stabilizing dendrite, as indicated by the presence of dendritic spines (Supplementary Movie 10), and distal dendrite dynamics (Supplementary Movie 11).[14b]

In summary, in this contribution we extend the utility of HIDE probes to achieve exceptionally long time-lapse images of the plasma membrane via STED nanoscopy. HIDE probes such as DiI-SiR are compatible with cultured (HeLa) and primary (hippocampal neurons) live cells, and the combination of high labeling density with a dark state reservoir enables the acquisition of significantly longer movies than with state-of-the-art fusion proteins while achieving high temporal resolution. We expect that the outstanding photostability of DiI-SiR will empower future studies of membrane dynamics. Ongoing work in our group is focused on applying DiI-SiR to long-term 3D and two-color nanoscopy in a variety of cell lines and utilizing next generation fluorophores.[20]

Supplementary Material

Refer to Web version on PubMed Central for supplementary material.

Acknowledgments

This work was supported by the Wellcome Trust (095927/A/11/Z) and in part by the NIH GM 83257 to A.S., GM 118486 to D.K.T., NS089662 to A.J.K., and S10 OD020142 (Leica SP8). A.D.T. and M.H.O. were supported by NIH Ruth L. Kirschstein NRSA F31GM119259 and F31NS090767, respectively. We thank Al Mennone (Yale University School of Medicine) for assistance with STED microscopy.

References

1. Abbe E. Arch Mikroskop Anat. 1873; 9:413–420.
2. a) Hell SW. Science. 2007; 316:1153–1158. [PubMed: 17525330] b) Huang B, Babcock H, Zhuang XW. Cell. 2010; 143:1047–1058. [PubMed: 21168201] c) Toomre D, Bewersdorf J. Annu Rev Cell Dev Bi. 2010; 26:285–314.
3. a) Liu Z, Lavis LD, Betzig E. Mol Cell. 2015; 58:644–659. [PubMed: 26000849] b) van de Linde S, Heilemann M, Sauer M. Annu Rev Phys Chem. 2012; 63:519–540. [PubMed: 22404589]
4. Quinn P, Griffiths G, Warren G. J Cell Biol. 1984; 98:2142–2147. [PubMed: 6563038]

5. Hell SW, Wichmann J. *Opt Lett*. 1994; 19:780–782. [PubMed: 19844443]
6. Erdmann RS, Takakura H, Thompson AD, Rivera-Molina F, Allgeyer ES, Bewersdorf J, Toomre D, Schepartz A. *Angew Chem Int Edit*. 2014; 53:10242–10246.
7. Takakura H, Zhang Y, Erdmann RS, Thompson AD, Lin Y, McNellis B, Rivera-Molina F, Uno S-n, Kamiya M, Urano Y, Rothman JE, Bewersdorf J, Schepartz A, Toomre D. *Nat Biotech*. 2017 advance online publication.
8. Lukinavicius G, Umezawa K, Olivier N, Honigmann A, Yang GY, Plass T, Mueller V, Reymond L, Correa IR, Luo ZG, Schultz C, Lemke EA, Heppenstall P, Eggeling C, Manley S, Johnsson K. *Nat Chem*. 2013; 5:132–139. [PubMed: 23344448]
9. Takakura H, Zhang Y, Erdmann RS, Thompson AD, Lin Y, McNellis B, Rivera-Molina F, Uno SN, Kamiya M, Urano Y, Rothman JE, Bewersdorf J, Schepartz A, Toomre D. *Nature Biotechnology*. 2017 In press.
10. Uno SN, Kamiya M, Yoshihara T, Sugawara K, Okabe K, Tarhan MC, Fujita H, Funatsu T, Okada Y, Tobita S, Urano Y. *Nat Chem*. 2014; 6:681–689. [PubMed: 25054937]
11. Miesenbock G, De Angelis DA, Rothman JE. *Nature*. 1998; 394:192–195. [PubMed: 9671304]
12. Kucic I, Rivera-Molina F, Toomre D. *Cilia*. 2016; 5:23. [PubMed: 27493724]
13. Stone DM, Hynes M, Armanini M, Swanson TA, Gu QM, Johnson RL, Scott MP, Pennica D, Goddard A, Phillips H, Noll M, Hooper JE, deSavauge F, Rosenthal A. *Nature*. 1996; 384:129–134. [PubMed: 8906787]
14. a) Dailey ME, Smith SJ. *J Neurosci*. 1996; 16:2983–2994. [PubMed: 8622128] b) Dotti CG, Sullivan CA, Banker GA. *J Neurosci*. 1988; 8:1454–1468. [PubMed: 3282038] c) Koleske AJ. *Nat Rev Neurosci*. 2013; 14:536–550. [PubMed: 23839597]
15. a) Westphal V, Rizzoli SO, Lauterbach MA, Kamin D, Jahn R, Hell SW. *Science*. 2008; 320:246–249. [PubMed: 18292304] b) Lauterbach MA, Keller J, Schonel A, Kamin D, Westphal V, Rizzoli SO, Hell SW. *J Biophotonics*. 2010; 3:417–424. [PubMed: 20379984] c) Urban NT, Willig KI, Hell SW, Nagerl UV. *Biophys J*. 2011; 101:1277–1284. [PubMed: 21889466] d) Nagerl UV, Willig KI, Hein B, Hell SW, Bonhoeffer T. *P Natl Acad Sci USA*. 2008; 105:18982–18987. e) Berning S, Willig KI, Steffens H, Dibaj P, Hell SW. *Science*. 2012; 335:551–551. [PubMed: 22301313] f) Lauterbach MA, Guillon M, Desnos C, Khamsing D, Jaffal Z, Darchen F, Emiliani V. *Neurophotonics*. 2016;3. g) Chereau R, Saraceno GE, Angibaud J, Cattaert D, Nagerl UV. *P Natl Acad Sci USA*. 2017; 114:1401–1406. h) Chereau R, Tonnesen J, Nagerl UV. *Methods*. 2015; 88:57–66. [PubMed: 26070997] i) Tonnesen J, Katona G, Rozsa B, Nagerl UV. *Nat Neurosci*. 2014; 17:678–685. [PubMed: 24657968] j) Willig KI, Steffens H, Gregor C, Herholt A, Rossner MJ, Hell SW. *Biophys J*. 2014; 106:L01–L03. [PubMed: 24411266] k) D’Este E, Kamin D, Gottfert F, El-Hady A, Hell SW. *Cell Rep*. 2015; 10:1246–1251. [PubMed: 25732815] l) Grunwald C, Schulze K, Giannone G, Cognet L, Lounis B, Choquet D, Tampe R. *J Am Chem Soc*. 2011; 133:8090–8093. [PubMed: 21545135] m) Lukinavicius G, Reymond L, D’Este E, Masharina A, Gutfert F, Ta H, Guether A, Fournier M, Rizzo S, Waldmann H, Blaukopf C, Sommer C, Gerlich DW, Arndt HD, Hell SW, Johnsson K. *Nat Methods*. 2014; 11:731–733. [PubMed: 24859753] n) Lauterbach MA, Guillon M, Soltani A, Emiliani V. *Sci Rep-Uk*. 2013;3. o) Wijetunge LS, Angibaud J, Frick A, Kind PC, Nagerl UV. *J Neurosci*. 2014; 34:6405–6412. [PubMed: 24790210]
16. a) Ondrus AE, Lee HLD, Iwanaga S, Parsons WH, Andresen BM, Moerner WE, Du Bois J. *Chem Biol*. 2012; 19:902–912. [PubMed: 22840778] b) Shim SH, Xia CL, Zhong GS, Babcock HP, Vaughan JC, Huang B, Wang X, Xu C, Bi GQ, Zhuang XW. *P Natl Acad Sci USA*. 2012; 109:13978–13983. c) Izeddin I, Specht CG, Lelek M, Darzacq X, Triller A, Zimmer C, Dahan M. *Plos One*. 2011;6. d) Ries J, Kaplan C, Platonova E, Eghlidi H, Ewers H. *Nat Methods*. 2012; 9:582–584. [PubMed: 22543348] e) Marriott G, Mao S, Sakata T, Ran J, Jackson DK, Petchprayoon C, Gomez TJ, Warp E, Tulyathan O, Aaron HL, Isacoff EY, Yan YL. *P Natl Acad Sci USA*. 2008; 105:17789–17794. f) Zhong GS, He J, Zhou RB, Lorenzo D, Babcock HP, Bennett V, Zhuang XW. *Elife*. 2014;3.
17. Maglione M, Sgrist SJ. *Nat Neurosci*. 2013; 16:790–797. [PubMed: 23799471]
18. Goodman CS. *Annu Rev Neurosci*. 1996; 19:341–377. [PubMed: 8833447]
19. a) Lefebvre JL, Kostadinov D, Chen WSV, Maniatis T, Sanes JR. *Nature*. 2012; 488:517–521. [PubMed: 22842903] b) Lefebvre JL, Sanes JR, Kay JN. *Annu Rev Cell Dev Bio*. 2015; 31:741–

777. [PubMed: 26422333] c) Zipursky SL, Grueber WB. *Annu Rev Neurosci.* 2013; 36:547–568. [PubMed: 23841842]
20. a) Butkevich AN, Mitronova GY, Sidenstein SC, Klocke JL, Kamin D, Meineke DN, D'Este E, Kraemer PT, Danzl JG, Belov VN, Hell SW. *Angew Chem Int Ed Engl.* 2016; 55:3290–3294. [PubMed: 26844929] b) Butkevich AN, Belov VN, Kolmakov K, Sokolov VV, Shojaei H, Sidenstein SC, Kamin D, Matthias J, Vlijm R, Engelhardt J, Hell SW. *Chem Eur J.* 2017; 23:1–7. c) Grimm JB, English BP, Chen JJ, Slaughter JP, Zhang ZJ, Revyakin A, Patel R, Macklin JJ, Normanno D, Singer RH, Lionnet T, Lavis LD. *Nat Methods.* 2015; 12:244–249. [PubMed: 25599551]

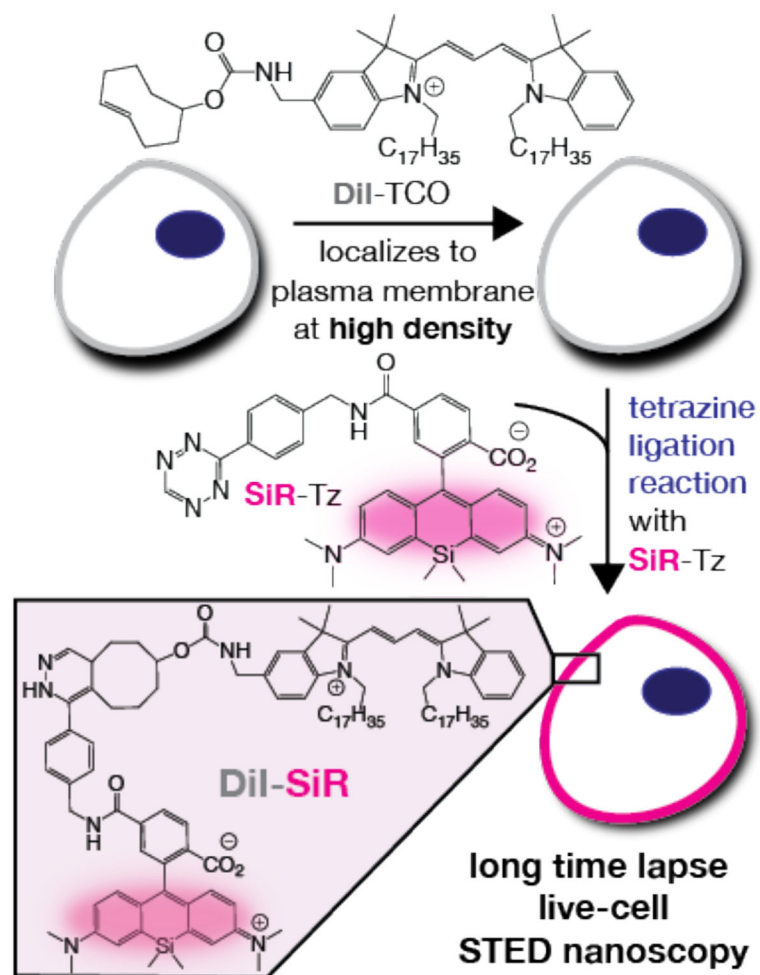
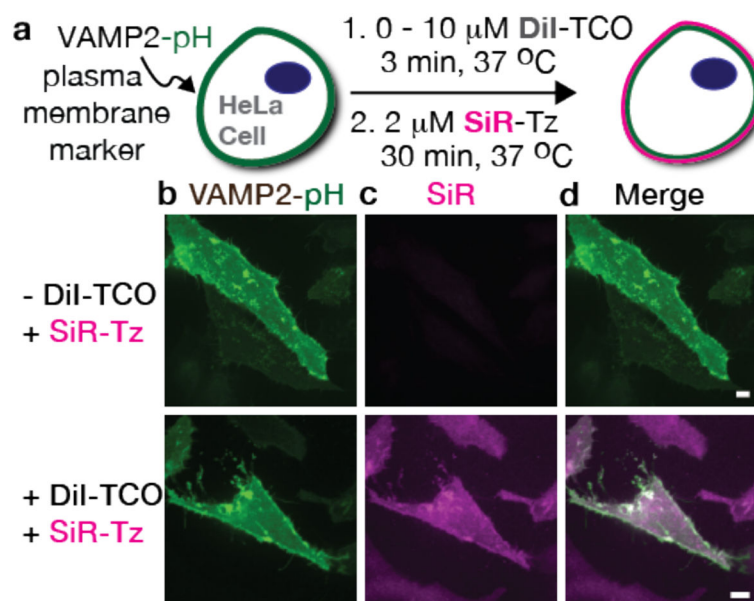


Figure 1. Two-step procedure to label the plasma membrane of live cells with the HIDE probe DiI-SiR. In the first step, DiI-TCO is localized to the plasma membrane (10 μ M DiI-TCO, 3 min at 37 $^{\circ}$ C); labelling occurs in a second step upon reaction of DiI-TCO with SiR-Tz (2 μ M; 30 min at 37 $^{\circ}$ C).

**Figure 2.**

DiI-SiR colocalizes with the plasma membrane marker VAMP2-pH. a) HeLa cells transiently expressing VAMP2-pH are treated at 37 $^{\circ}\text{C}$ with 0 or 10 μM DiI-TCO for 3 min followed by 2 μM SiR-Tz for 30 min and the cells visualized using confocal microscopy. Confocal images obtained by detecting the (b) VAMP2-pH channel or (c) the SiR channel of cells treated with SiR-Tz and with or without DiI-TCO. d) Merge of the VAMP2-pH and SiR channels of cells treated with SiR-Tz and with or without DiI-TCO. Scale bars: 10 μm .

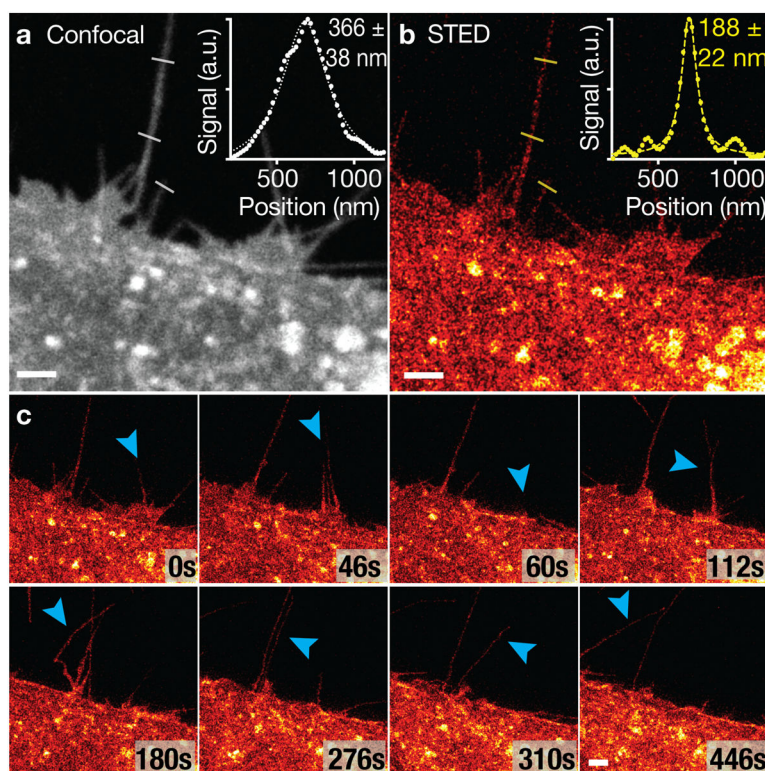
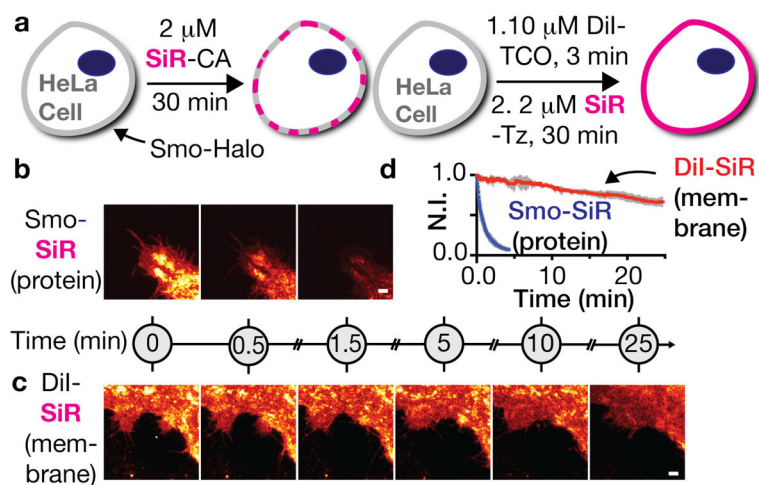


Figure 3.

Long time-lapse STED imaging of live HeLa cells labeled with DiI-SiR. HeLa cells are treated at 37 °C with 10 μ M DiI-TCO for 3 min followed by 2 μ M SiR-Tz for 30 min and the cells visualized using a Leica SP8 STED microscope. a) Confocal image of filopodia. The average signal from the 3 line profiles shown (white lines) appears as an insert. A fit of this data to a Lorentzian function (white dotted line) provides a FWHM (mean \pm SD, $n = 3$) of 366 ± 38 nm. b) STED image of filopodia. A fit of the 3 line profiles shown (yellow lines) to a Lorentzian function (yellow dotted line) provides a FWHM value (mean \pm SD, $n = 3$) of 188 ± 22 nm. c) Time-lapse images of HeLa cell dynamics. Blue arrows indicate filopodia movement. Scale bars: 2 μ m.

**Figure 4.**

Comparison between Smo-Halo and DiI-SiR labeling in live HeLa cells. a) HeLa cells transiently expressing Smo-Halo are treated at 37 °C with 2 μM SiR-CA for 30 min and compared to HeLa cells treated at 37 °C with 10 μM DiI-TCO for 3 min and 2 μM SiR-Tz for 30 min. b,c) Time course images of cells labeled with Smo-SiR or DiI-SiR imaged under the same conditions using a Leica SP8 STED microscope. Time line shown in minutes with breaks to show later time points. b) STED imaging of Smo-SiR over time. c) STED imaging of DiI-SiR over time. d) Plot of the normalized fluorescence intensity of Smo-SiR (blue) and DiI-SiR (red) over time (mean ± SD, n = 3 cells). Scale bars: 2 μm.

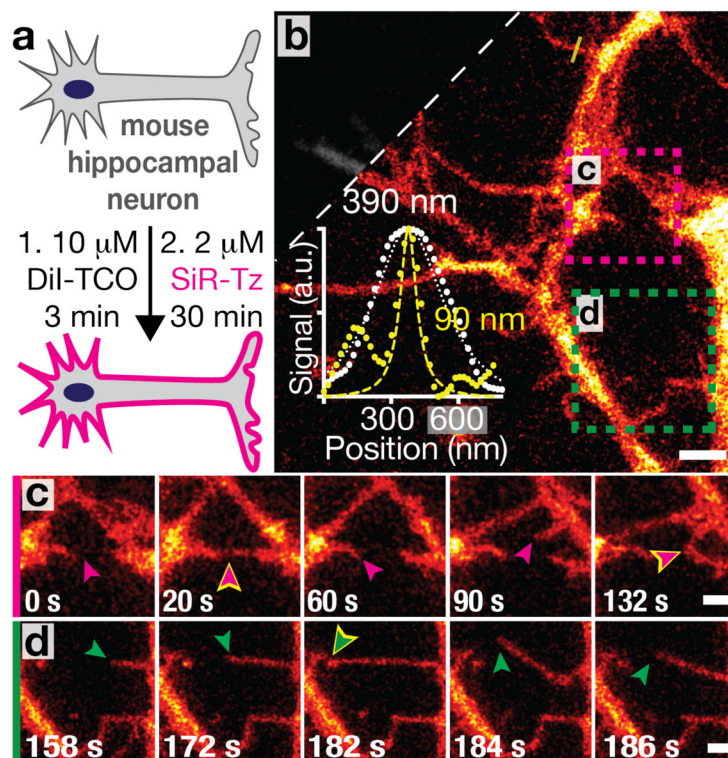


Figure 5. Long-term live-cell STED imaging of DIV 4 mouse hippocampal neurons with DiI-SiR. a) DIV 4 neurons were labeled with $10\ \mu\text{M}$ DiI-TCO for 3 min followed by $2\ \mu\text{M}$ SiR-Tz for 30 min. b) Snapshot of a STED movie with confocal cutaway in gray. The yellow line profile is shown as an insert. The dashed yellow line represents the Lorentzian fit for the STED image, while the white dotted line represents the Lorentzian fit for the confocal image. These profiles are characterized by FWHM values of 90 nm (STED) and 390 nm (confocal). c) Pink, and d) green square outline from b; timecourses with corresponding pink and green arrows denoting filopodia dynamics; yellow outlines designate contact events. Scale bars: $2\ \mu\text{m}$ in b, $1\ \mu\text{m}$ in c,d.